A PRACTICAL LOOK AT MONTE CARLO VARIANCE REDUCTION METHODS IN RADIATION SHIELDING

RICHARD H. OLSHER
Health Physics Measurements Group, Los Alamos National Laboratory
MS J573, P.O. Box 1663, Los Alamos, NM 87545 USA
E-mail : dick@lanl.gov

Received December 16, 2006

With the advent of inexpensive computing power over the past two decades, applications of Monte Carlo radiation transport techniques have proliferated dramatically. At Los Alamos, the Monte Carlo codes MCNP5 and MCNPX are used routinely on personal computer platforms for radiation shielding analysis and dosimetry calculations. These codes feature a rich palette of variance reduction (VR) techniques. The motivation of VR is to exchange user efficiency for computational efficiency. It has been said that a few hours of user time often reduces computational time by several orders of magnitude. Unfortunately, user time can stretch into the many hours as most VR techniques require significant user experience and intervention for proper optimization. It is the purpose of this paper to outline VR strategies, tested in practice, optimized for several common radiation shielding tasks, with the hope of reducing user setup time for similar problems. A strategy is defined in this context to mean a collection of MCNP radiation transport physics options and VR techniques that work synergistically to optimize a particular shielding task. Examples are offered in the areas of source definition, skyshine, streaming, and transmission.

KEYWORDS : Monte Carlo, Radiation Transport, Variance Reduction, Photon Skyshine, Bremsstrahlung Conversion, Maze Streaming, Weight Window Generator

I. INTRODUCTION

With the advent of inexpensive computing power over the past two decades, applications of Monte Carlo radiation transport techniques have proliferated dramatically. At Los Alamos, the Monte Carlo codes MCNP5 [1] and MCNPX [2] are used routinely on personal computer platforms for radiation shielding analysis and dosimetry calculations. These codes are attractive for such applications because of their ability to accommodate complex 3-D geometries, inclusion of flexible physics models that provide coupled electron-photon and neutron-photon transport, and the availability of extensive continuous-energy cross section libraries derived from evaluated nuclear data files. It should be noted that these codes are general purpose in nature, and are therefore not optimized for any particular application. It is left up to the user to select appropriate variance reduction (VR) tools from a rich palette of such tools bundled with these codes.

An excellent overview of classic MCNP VR techniques was given by Booth [3]. Recent developments such as the weight window generator and automated VR using deterministically generated importance functions have been described by several authors [4,5,6,7,8,9]. Both the A^3MCNP patch to the MCNP code [7] and the stand-alone code ADVANTAG [6] appear to greatly improve the computational efficiency for deep penetration problems.

The efficiency of a Monte Carlo simulation may be quantified using the Figure of Merit (FOM), which is defined by the MCNP code developers according to Equation 1, where R is the tally relative error and T is the computing time.

$$\mathrm{FOM} = \frac{1}{R^2 T} \tag{1}$$

For a fixed computing time, the smaller the variance- the larger the FOM. It should be noted that R^2 is proportional to 1/N, where N is the total number of histories, and T is proportional to N. Thus, for a well converged simulation, the FOM becomes constant.

The motivation of VR is to exchange user efficiency for computational efficiency. It has been said that a few hours of user time often reduces computational time by several orders of magnitude. Unfortunately, user time can stretch into the many hours as most VR techniques require

significant user experience and intervention for proper optimization. It is the purpose of this paper to outline VR strategies, tested in practice, optimized for several common radiation shielding tasks, with the hope of reducing user setup time for similar problems. A strategy is defined in this context to mean a collection of MCNP radiation transport physics options and VR techniques that work synergistically to optimize a particular shielding task.

VR methods have been traditionally categorized into four basic types, as follows: truncation, population control, modified sampling, and partially deterministic methods. The truncation method, as the name implies, truncates parts of phase space (spatial extent, particle energy, direction, or time) that do not contribute to the solution. This is potentially a powerful method that can directly save computing time without introducing particle weight dispersion. However, the user must actively involve himself by invoking a-priori knowledge and experience to constrain problem parameters without biasing the simulation results. Truncation methods can be very effective, but user care is essential as there is always the potential of inadvertently truncating an essential region of phase space. The population control method typically uses particle splitting and Russian Roulette to control the sampling density in various regions of phase space. In modified sampling, the statistical sampling of a particular problem variable (or variables) is biased to increase the scoring efficiency. Finally, partially deterministic methods circumvent part of the normal random walk process to increase scoring efficiency. With the exception of truncation, these methods typically (but not always) increase computing time per history. Many roulette games are played in MCNP (weight window, weight cutoffs, DXTRAN and point detector contributions) for the expressed purpose of decreasing the computing time per history. Even if computing time increases slightly, the variance typically decreases faster than the increase in time, resulting in a net increase of the FOM.

It is useful to divide a radiation shielding analysis into four basic tasks: source definition, skyshine, streaming, and transmission. For a specific facility and source term, exposure pathways can be divided into skyshine through the roof of the shield enclosure, streaming through entrance mazes and shield penetrations, and transmission through the primary and secondary shield walls. Each task typically requires a unique VR strategy, which may conflict with the requirements for other tasks. This is not surprising since most VR games proceed along a preferred direction and optimize the solution for a specific exposure pathway and location. Examples will be given for each of these basic tasks.

2. SOURCE DEFINITION AND TRANSPORT PHYSICS OPTIONS

A bremsstrahlung conversion problem will be discussed in the context of a commercial electron linear accelerator (Varian M9 Linatron). A 9 MV mono-directional electron beam is incident on a thin tungsten target and it is desired to determine the forward x-ray spectrum for subsequent transmission calculations through a shield wall.

Most bremsstrahlung is produced early in the electron's random walk. As the electron slows down in the target, collisional losses eventually dominate over radiative losses, and any bremsstrahlung produced becomes softer and less likely to escape the target. For these reasons, it makes no sense to track electrons in the target down to the default cutoff energy of 1 keV. Since electron transport is very time consuming, a considerable computing time saving can be realized by setting a higher cutoff energy using either the cut:e or the elpt:e cards. The optimum cutoff energy (E_{cut}) is dependent on both the maximum electron beam energy (E_{max}) and the critical energy of the target (E_c). The critical energy is defined as that energy at which collisional and radiative stopping powers are equal. For a target of a given atomic number Z, the critical energy may be calculated by Eqn. 2.

$$E_c = \frac{800}{Z+2} \tag{2}$$

The electron cut off energy, E_{cut}, may be set as the smaller of the following expressions:

(a) $E_{cut} = 0.25E_{max}$
(b) $E_{cut} = 0.25E_c$

For tungsten (Z=74), E_{max} of 9 MeV and E_c of 10.53 MeV, the above expressions yield an electron cutoff energy of 2.25 MeV. As insurance against the possibility of bias, the user may select a slightly lower cutoff energy. An even safer approach is to substitute an energy roulette game for the electron cutoff with a very small survival probability (ESPLT:e 0.001 2.25). Electrons will undergo a roulette game as they are slowed down below 2.25 MeV, but some of these electrons will survive and possibly contribute to the tally.

In addition, for standard targets whose thickness is typically at least one-third of the maximum electronic range, it is recommended that the production of knock-on electrons (delta rays) be turned off on the phys:e card (phys:e 7j 0). The energy distribution of knock-on electrons is soft and therefore these secondary electrons contribute much less to the total x-ray production relative to the primary electrons. In addition, knock-on electron bremsstrahlung is more likely to be absorbed in the target.

It is also beneficial to bias bremsstrahlung photon production toward higher energies, to better sample the tail of the spectrum, since the high-energy portion of the spectrum is most important for shielding purposes. This

Table 1. 9MV Electron Linear Accelerator. Figure of Merit as a Function of Various Electron Transport Options. Air Kerma Rate is Given at 100 cm for 150 μA Electron Beam

Electron Transport Options	Air Kerma Rate (Gy/minute) (Relative Error %)	Figure of Merit
Electron E_{cut} = default (1 keV) Knock-on electron = YES	31.1 (0.95%)	11
Electron E_{cut} = default (1 keV) Knock-on electron = NO	31.2 (0.31%)	107
Electron E_{cut} = 0.1 MeV Knock-on electron = YES	31.2 (0.14%)	547
Electron E_{cut} = 2.25 MeV Knock-on electron = NO	31.0 (0.04%)	5936
Energy Roulette: ESPLT:e 0.001 2.25 Knock-on electron = NO	31.1 (0.28%)	131

can be done by invoking the bremsstrahlung biasing card (bbrem card), which not only increases the total probability of x-ray production but also allows for an increase in the bias factor with increasing photon energy.

In general, an array of point detectors may be positioned relative to the electron beam centerline to improve scoring efficiency and map out the photon beam's angular distribution. Since the M9 Linatron's x-ray beam was collimated within a 15-degree cone, an F4 tally type was defined over a thin cylindrical cell whose cross-sectional area was equal to that of the beam at a distance of 100 cm from the target. A DXTRAN sphere was centered over the tally cell to improve scoring efficiency. The average fluence was converted to air kerma using the ICRP-74 [10] conversion function. Tally results were normalized to a beam current of 150 μA. Several 1000-minute runs were performed on the same computer using various electron transport options. The results are summarized in Table 1. Reducing the amount of time spent on tracking low-energy electrons results in a major increase in the FOM. Most of the increase in efficiency results from increasing the electron cutoff energy. When E_{cut} is set as high as 0.25 E_e, the decrease in the air kerma rate is still less than 0.5% of that obtained with the default electron transport options. Use of an electron energy roulette game (instead of the cut card), even with a low survival probability of 0.001, is seen to be far less efficient relative to the cut card.

3. PHOTON SKYSHINE

To verify the accuracy of the MCNP code for skyshine simulations and to study optimum VR strategy, Olsher, Hsu, and Harvey [11] benchmarked its performance against the Kansas State University (KSU) photon skyshine experiment of 1977. In this experiment [12], ^{60}Co sources were either collimated into an upward 150-deg conical beam by means of a thick cylindrical concrete silo or shielded vertically by two different thicknesses of concrete. A NaI (Tl) spectrometer and a pressurized ion chamber were used to measure, respectively, the energy spectrum and the 4π-exposure rate of the air-scattered gamma photons up to 700 m from the source. The KSU experiment for the unshielded source geometry was simulated in great detail to include the contribution of groundshine, in-silo photon scatter, and the effect of spectral degradation in the source capsule. The standard deviation of the KSU experimental data was stated to be 7%, while the statistical uncertainty of the simulation was kept at or under 1%. The results of the simulation agreed closely with the experimental data, generally to within 6%. At distances of under 100 m from the silo, the modeling of the in-silo scatter was crucial to achieving close agreement with the experiment. Specifically, scatter off the top layer of the source cask accounted for approximately 12% of the dose at 50 m. At distances >300 m, using the ^{60}Co line spectrum led to a dose over response as great as 19% at 700 m. It was necessary to use the actual source spectrum, which includes a Compton tail from photon collisions in the source capsule, to achieve close agreement with experimental data. These simulations formed the basis for the following recommended VR strategy.

(a) Air space around the facility may be truncated to two mean free paths (mfp) – based on the maximum photon energy. In addition, each detector should be surrounded by at least one mfp of air. Since it is known that skyshine

dose is mostly due to the first-collision dose, there is no need to sample collision sites further removed from tally locations.

(b) Groundshine typically contributes about 20% of the total skyshine dose. Therefore, ground scatter should be taken into account via a suitable ground plane model, at least two mfp thick.

(c) Point detector tallies (Type 5) are ideal for this application, in that they force fluence contributions to be made from collision sites removed from the detector, thus greatly improving scoring efficiency. It is permissible to use point detectors in lightly scattering media – provided that a sphere of exclusion is defined around the detector to protect the tally from huge scores due to collision distances that approach zero. Assuming that the detectors are located at least 100 cm above the ground plane, a sphere of exclusion radius in the range of 50 to 100 cm works well in this application. If rotational symmetry exists in the facility, a set of ring detectors may be used to take advantage of that circumstance.

(d) Facility wall thickness may be truncated to about two mfp in extension to provide for an albedo effect, without tracking particles very deeply into the shield walls. Figure 1 shows a cross-sectional view of the KSU silo model. The interior region of the silo wall was defined as a zero importance cell or "kill zone" to accomplish these goals. Particle tracks that penetrated deeper than about two mfp into the interior of the wall were killed since transmission was not a viable exposure pathway.

(e) The PD card should be used to control point detector contributions on a per cell basis. For example, any source cell for which uncollided source contributions traverse a zero importance region, should be assigned a value of PDn nearly equal to zero to inhibit direct contributions to tally number n. For example, a value of 0.01 represents a safer choice than zero as it eliminates the possibility of ignoring collided particles that the user mistakenly thought could not contribute to the detector from within a given cell.

(f) Coherent Scatter should be turned off using the photon physics card (phys:p 2j 1) to improve point detector tally convergence.

4. PHOTON TRANSMISSION AND STREAMING THROUGH A MAZE

A maze entrance is used routinely in industrial and medical facility design to obviate the need for a heavy and expensive movable door. The maze walls are typically sufficiently thick to eliminate transmission as a concern, leaving streaming through the maze opening as the primary exposure pathway. Figure 2 shows a facility floor plan incorporating a maze, which will be used in the following discussion. All of the walls and floor slab are concrete specified as ANSI composition [13]; the walls are 60 cm thick while the floor slab is 10 cm thick. The facility lacks a roof shield, therefore all air spaces were made void to eliminate the contribution of skyshine to the tally. The source is a point isotropic source of ^{137}Cs photons located at a height of 150 cm off the floor. A point detector was located at the exterior entrance, at the center of the opening, at a height of 100 cm above the floor. In addition, a DXTRAN sphere were used to increase the number of photons entering the maze – as shown in Fig. 2. This VR technique provides angular biasing at source and collision events toward the solid angle defined by the sphere and allows for either better sampling of spatial regions within the sphere or, as in this case, increased sampling of important particle

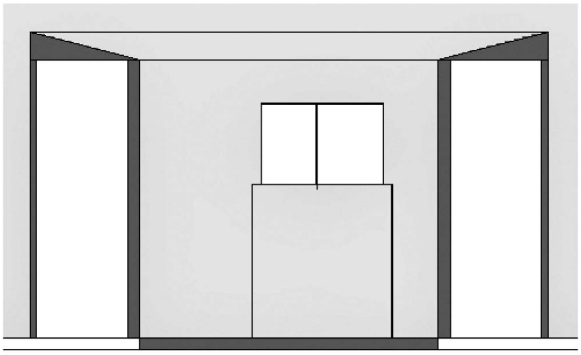

Fig. 1. Cross-sectional View of the KSU Cylindrical Concrete Silo Showing the Location of the Source Casks. The Light Area Interior to the Wall is a "Kill zone" - Assigned an Importance of Zero

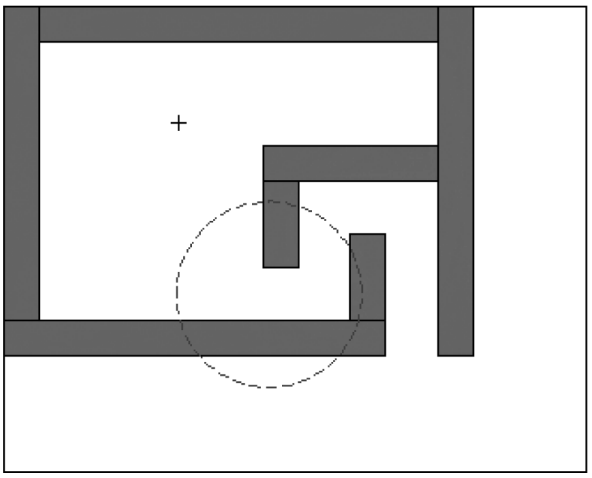

Fig. 2. Maze Floor Plan Showing Location of Source (+). Dashed Circle Denotes Location of DXTRAN Sphere in the Analysis

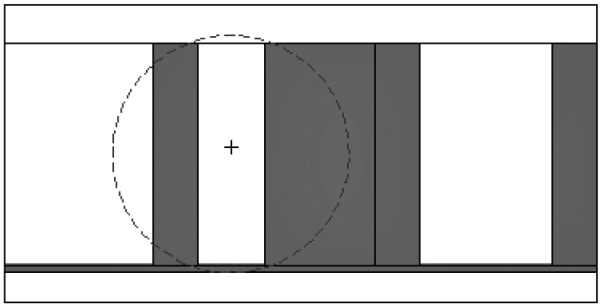

Fig. 3. Maze Elevation View. Dashed Circle Denotes Overlay of DXTRAN Sphere at the Maze Interior Entrance – as Used in the Analysis

directions. While angular biasing represents an important aspect of this game which focuses on increasing tally contributions, from a VR viewpoint it is more important to think of DXTRAN as a "shield" against large-weight detector contributions. Ideally, the DXTRAN sphere should be sized such that it fills the rectangular opening of the maze. When there are gaps between the DXTRAN sphere and maze walls, high-weight non-DXTRAN particles could potentially enter the maze by streaming around the sphere. The benefits of pulling a larger number of low-weight DXTRAN particles into the maze can be destroyed by a few high-weight non-DXTRAN particles streaming around the sphere. As can be seen in Fig. 3, the diameter of the sphere was adjusted to completely fill the interior maze opening, which is rectangular in shape.

The maze problem was investigated using mesh-based weight windows. When used in conjunction with DXTRAN, it is possible to optimize the importance function for the simulation of both transmission and streaming. The MCNP Weight Window Generator (WWG) makes it possible to generate an importance function with respect to both an energy grid and a spatial grid that overlays the existing geometry. Particle splitting and Russian roulette may then be played as a function of both particle position and energy. It is well known that the WWG is statistical in nature. The importance of each cell is defined as the ratio of the total score resulting from particles (and their progeny) that enter a cell to the total weight that entered the same cell. For deep penetration problems (e.g., the walls of the maze), it becomes very difficult to obtain reliable importance estimates for many mesh elements because they are not visited at all, or visited rarely, during the random walk In the past several years, much work has been directed towards automatically generating deterministic importance functions for use in MCNP. Recent work at Los Alamos by Sweezy at al [9] has focused on using adjoint flux solutions from the PARTISN 3D discrete ordinates code to generate weight windows for MCNP5. It is hoped that in the future such capability will become a standard feature in MCNP.

In the interim, it is possible to enhance the performance of the standard WWG for deep penetration problems by using it in conjunction with the exponential transform and/or a density reduction technique to produce a reasonable initial (first generation) importance

Table 2. Maze Streaming Simulations Using Mesh-based Importance Functions, Geometry as Shown in Figs. 2 and 3. First Generation Importance Function was Derived from a 20-minute Run at Reduced Concrete Density

Simulation Type	Fluence (cm^{-2}) per source photon (Relative Error %)	Figure of Merit	H*(10) (pSv per source photon) (Relative Error %)	Figure of Merit
DXTRAN 1st generation importance function	1.56E-10 (0.74%)	30	9.69E-11 (0.72%)	32
DXTRAN 2nd generation importance function	1.57E-10 (0.18%)	500	9.76E-11 (0.19%)	453
DXTRAN 3rd generation importance function	1.57E-10 (0.18%)	524	9.79E-11 (0.19%)	483
NO DXTRAN 4th generation importance function	1.57E-10 (0.25%)	274	9.75E-11 (0.25%)	275

function. Collisions deep within the shield walls, near the point detector, contribute the largest scores. Unfortunately, the fluence falls off exponentially with depth into the shield, so that these important collisions are inadequately sampled for deep penetration problems. In particular, the density reduction technique was applied to the maze problem to produce an initial importance function during a short 20-minute run, which included one DXTRAN sphere as shown in Figs. 2 and 3. This technique is based on the principle that the importance function is independent of the global fill density used for the shield walls. Therefore, by reducing the wall density from its natural value of 2.3 g/cm^3 by a factor of 10 to 0.23 g/cm^3, the wall's optical thickness is reduced from about 15 mean free paths (mfp) to 1.5 mfp, ensuring that particle tracks visit cells deep within the shield walls.

A rectangular mesh was defined with a spatial resolution of 25 cm along the x and y axes, and about 30 cm along the z axis. The importance function was generated in two energy bins (<0.1 and 0.1 - 1 MeV). Use of the initial importance function (600 minute run), with the shield density reset to its natural value, produced a reasonable FOM. The WWG was left on during this run, producing a second generation importance function. All subsequent simulations were performed at identical run times on the same personal computer, and with the WWG generator left on.

The second generation importance function proved sufficiently accurate to produce an impressive increase in the FOM – over an order of magnitude relative to the first generation function. The third generation importance function only resulted in a minor increase in the FOM. No further attempt was made to improve the simulation efficiency through the use of PD and DXC cards. An additional simulation was performed with the fourth generation importance function but with the DXTRAN VR turned off. In this case, the FOM decreased by almost a factor of two. The mesh-based importance function maze simulations are summarized in Table 2.

5. CONCLUSIONS

The MCNP/MCNPX code family offers a rich palette of VR techniques. Several successful VR strategies have been outlined with the aim of reducing user setup time for common radiation shielding tasks. In particular, the benefit of using the WWG to create importance functions was investigated. It was shown that the density reduction technique can be used effectively to improve the performance of the WWG for deep penetration and maze streaming problems. This technique can generate a decent first generation importance function and that the second generation function derived from the initial estimate can result in excellent computational efficiency.

ACKNOWLEDGEMENT

The author would like to thank Dr. Thomas E. Booth of the Los Alamos National Laboratory for his critical review of the manuscript and helpful comments and suggestions.

REFERENCES

[1] MCNP Monte Carlo Team, X-5, *MCNP5_RSICC_1.30, LA-UR-04-5921*, Los Alamos National Laboratory, Los Alamos, NM (2004).

[2] J. S. Hendricks, G. W. McKinney, L. S. Waters, et al., *MCNPX, Version 2.5.e, LA-UR-04-0569*, Los Alamos National Laboratory, Los Alamos, NM (2004).

[3] T.E. Booth, "A Sample Problem in Variance Reduction in MCNP," Los Alamos National Laboratory, LA-10363-MS (1985).

[4] K.A. Van Riper, T.J. Urbatsch, P.D. Soran, D.K. Parsons, J.E. Morel, G.W. McKinney, S.R. Lee, L.A. Crotzer, F.W. Brinkley, T.E. Booth, J.W. Anderson, and R.E. Alcouffe, "AVATAR – Automatic Variance Reduction in Monte Carlo Calculations," LA-UR-97-0919, Los Alamos National Laboratory (1997).

[5] J.C. Wagner and A. Haghighat, "Automated Variance Reduction of Monte Carlo Shielding Calculations Using the Discrete Ordinates Adjoint Function," *Nucl. Science and Eng.*, **128**, 186 (1998).

[6] J.C. Wagner, "An Automated Deterministic Variance Reduction Generator for Monte Carlo Shielding Applications," *Proc. American Nuclear Society, Rad. Prot. Division, 12th Topical Meeting*, Santa Fe, NM USA, Apr.14-18,2002.

[7] A. Haghighat and J.C. Wagner, "Monte Carlo Variance Reduction with Deterministic Importance Functions," Progress in Nuclear Energy, 42(1), 25-53 (2003).

[8] H.P. Smith and J.C. Wagner, "A Case Study in Manual and Automated Monte Carlo Variance Reduction with a Deep Penetration Reactor Shielding Problem," *Proc. Nucl. And Comp. Sciences: A Century in Review, A Century Anew*, Gatlinburg, TN, USA, Apr. 6-11,2003.

[9] J. Sweezy, T. Booth, F. Brown, J. Chiaramonte, and W. Preeg, "Automated Variance Reduction for MCNP using Deterministic Methods," LA-UR-04-3133, Los Alamos National Laboratory (2004).

[10] International Commission on Radiological Protection. ICRP Report 74. *Conversion Coefficients for use in Radiological Protection Against External Radiation* (1998).

[11] R.H. Olsher, H.H. Hsu, and W.F. Harvey, "Benchmarking the MCNP Monte Carlo Code with a Photon Skyshine Experiment," *Nucl. Science and Eng.*, **114**, 219-226 (1993).

[12] R. R. Nason, J.K. Shultis, R.E. Faw, C.E. Clifford, "Benchmark Gamma Ray Skyshine Experiment," *Nucl. Science and Eng.*, **79**, 404-416 (1981).

[13] American National Standard ANSI/ANS-6.6.1-1987. "Calculation and Measurement of Direct and Scattered Gamma Radiation from LWR Nuclear Power Plants (1987).